Building and Environment 183 (2020) 107049

Contents lists available at ScienceDirect

Building and Environment

journal homepage: http://www.elsevier.com/locate/buildenv

Monitorization and statistical analysis of south and west green walls in a retrofitted building in Madrid

R. Sendra-Arranz [a,*], V. Oquendo [b,c], L. Olivieri [b,c], F. Olivieri [b,c], C. Bedoya [b,c], A. Gutiérrez [a,c]

[a] E.T.S. Ingenieros de Telecomunicación, Universidad Politécnica de Madrid, Av. Complutense 30, 28040, Madrid, Spain
[b] E.T.S. Arquitectura, Universidad Politécnica de Madrid, Av. Juan de Herrera 4, 28040, Madrid, Spain
[c] Innovation and Technology for Development Center, Universidad Politécnica de Madrid, Av. Complutense, 28040, Madrid, Spain

ARTICLE INFO

Keywords:
Green walls
Green façades
Monitoring system
Exploratory data analysis

ABSTRACT

Green walls can act as natural thermal regulators, reducing solar radiation on surfaces and providing cooling due to shading and evapotranspiration. Several studies have investigated the cooling effects of a bare wall, in contrast to a vegetated wall, as well as the correlation between temperature reduction and system characteristics. In the present work, we analyze the influence of the orientation of a green wall on its ability to reduce surface temperatures in a Mediterranean climate. Environmental variables such as irradiation and air temperature have been considered. A real-time monitoring system has been used, with a database of three years of measurements. Results show that on average, the control temperature is greater than the green wall temperature with maximum differences of 20 °C in summer and 8 °C in winter in the south wall surface. During the summer, the temperature reduction in the south façade occurs mainly in the central hours of the day, while in the west façade it occurs mainly in the afternoon. Being the summer the most relevant season for the use of green walls, this information is very valuable as it allows the designers to know at what time of day the façade provides a temperature reduction, depending on the orientation.

1. Introduction

The impacts of urbanization and climate change are driving a transformation towards complex scenarios that threaten the sustainability of the planet [1]. The world population is constantly growing, using unrenewable natural resources in a continuous and unbalanced way. The consequences of climate change are becoming increasingly visible alongside this scenario: rising temperatures, floods, droughts, air pollution, noise, etc. These effects, in addition to harming life inside cities, diminish the development of new plant species, degrade habitats, alter the development of species adapted to a particular type of climate and reduce drinking water reserves, among others [2]. Currently cities are at the centre of political, social and environmental decision-making.

Mitigating and adapting cities to the effects of climate change means coping with the expected and widespread effects. It is estimated that more than half of the world population will live in cities by 2050, equivalent to 90% development of urban contexts [1]. In other words, urban growth will be approximately one million people per week. Nowadays, cities represent 3% of the earth's surface, and paradoxically are responsible for 80% of the energy consumption and about 75% of CO_2 emissions into the atmosphere. This is a reflection on the fact that population growth will not only be synonymous of urbanization but also of high consumption and pollution ratios [3,4].

This scenario has been the starting point for global initiatives such as Agenda 2030 and the Sustainable Development Goals (SDGs) [5]. 193 member states of the United Nations unanimously adopted a route composed of 17 SDGs based on three main dimensions: society, environment, and economy. This new approach has changed how human development problems are addressed. It will require tackling challenges on a global scale and in an increasingly complex and interdependent world that requires significant resource management. To achieve these challenges in a stable and long-term scenario, transformations and incentives are needed to promote resilient technologies that stimulate current governance mechanisms.

Considering the challenges of climate change as opportunities for innovation, nature-based solutions can be part of new technologies aimed at preserving biodiversity and solving economic, social and environmental problems. The nature-based solution term emerged in

* Corresponding author.
E-mail addresses: r.sendra@alumnos.upm.es (R. Sendra-Arranz), valentina.oquendo@upm.es (V. Oquendo), lorenzo.olivieri@upm.es (L. Olivieri), francesca.olivieri@upm.es (F. Olivieri), cesar.bedoya@upm.es (C. Bedoya), a.gutierrez@upm.es (A. Gutiérrez).

https://doi.org/10.1016/j.buildenv.2020.107049
Received 9 March 2020; Received in revised form 24 May 2020; Accepted 7 June 2020
Available online 6 July 2020

2000 as the relationship between nature and people. It primarily focuses on the benefits that nature can bring to environmental and social challenges such as climate change. On the other hand, the European Commission defines them as “those that can turn nature into opportunities for social, economic, and environmental innovation” [6]. For example, through complex natural processes such as the absorption of carbon dioxide, the treatment and management of rainwater or the fixation of atmospheric particles, among others, succeed in reducing environmental risks and achieving human well-being. Nature-based solutions should be developed through four main objectives and seven actions to be developed in the field of research and innovation, highlighting the importance of their implementation to increase the resilience of urban environments.

The idea that nature brings benefits to city life and society as a whole has been developed in different contexts. All of them focusing on sustainability and the capacity to provide provisioning, regulation, and recreation services. It has also been contemplated and disseminated through environmental policies and initiatives of recent decades, shaping research programs that have incorporated this discourse aligning it with the SDGs, especially the SDG 11 “Make cities and human settlements inclusive, safe, resilient and sustainable”. According to this SDG, this paper focuses on investigating green walls as nature-based solutions to reduce temperatures in dense urban environments. More precisely, it focuses on analyzing the behavior of a vegetal façade in two orientations (south and west).

Greening the building envelope allows obtaining some benefits related to the improvement of building efficiency and its ecological and environmental performance. Green walls, as part of vertical greening solutions, are the result of the integration of vegetation on buildings aiming at improving air quality [7], related to the reduction of fine dust levels [8], increase of biodiversity [9], reduction of heat island effect in urban areas [10], and the reduction of energy consumptions for cooling and heating [11]. The benefits of these solutions can be synthesized as the influence of substrate and vegetation thickness, water content, air cavity between the various layers, and the materials used for their construction [12].

Within the classification of vegetal façades, there is a wide range of technical solutions characterized by vertical support structures that may be attached or not to the façade of a building. Depending on the type of the system, there are different configurations. They range from quite simple ones, such as those with vertical support to the more technologically and complex such as the modular ones. Nevertheless, the dimensional and material characteristics between the systems within the same classification are usually the same. A vegetal façade system is composed of fixed (or primary) and variable (or secondary) elements that are determined based on the complexity of the project. As primary components there are supporting elements, water absorption, retention elements, substrates, vegetation and irrigation and fertilisation systems. Second components create vapor barrier layers, insulating layers, vapor pressure diffusion layers and separation layers of different materials [13–17].

Modular façade systems emerge as an innovative solution for incorporating vegetation into building envelopes [12]. Their configuration and the pre-cultivation of plants allow the instantaneous coverage of large vertical surfaces, being an adaptable solution to any type of building. In this category, different solutions, that vary by composition, module dimensions, substrate type, number of plants per module and support material, can be developed in the form of trays, three-dimensional structures, containers or geotextile bags (see Fig. 1).

The trend towards construction with materials such as concrete, glass, and metals is one of the causes of the phenomenon of the urban heat island. This type of surface reflects the solar radiation incident to their immediate surroundings, generating a significant increase in temperatures [18]. It has implications for the energy balance of buildings, as well as problems related to public health [19]. Most of the solutions developed in the last decades include the implementation of high albedo materials [20], which guarantees the rebound of sunlight reflected on the surface to the radiation that affects it. This group of solutions includes green roofs, due to the ability of plants to absorb irradiation and use it in their natural biological processes [21]. The current market and most of the research have concentrated on solving the problem from horizontal surfaces [19,22–25]. However, few have stressed the importance of vertical surfaces in the comfort of the urban mesh.

The vegetation in walls can contribute to the improvement of the microclimate in cities both inside and outside buildings. It is a mitigation strategy due to its function as a natural regulator against the temperatures reached because of the climate change. In dense urban environments, vegetation can contribute to cooling the air and providing shade [26]. It can also be a passive energy efficiency strategy, as it acts as an isolating layer on building façades. These benefits have been extensively studied and linked to the ability of the foliar apparatus to reduce wind speed, the thermal inertia of the substrate, and the ability to regulate temperatures through moisture added to the air by evapotranspiration [26–31].

Wong et al. [32] conducted a research to identify the influence of different vertical green systems on the urban microclimate. Results showed a reduction of up to 3.3 °C at a distance of up to 15 cm due to the effect of evapotranspiration. Likewise Perini et al. [33], studied the behavior of three façades of different plants and their incidence on the air temperature. They demonstrate similar results for the three systems, which highlights the benefits of vegetation regardless of their constructive configuration. The results of Tabassom et al. [34], demonstrate the behavior of vertical green in humid and warm climates such as Malaysia, with reductions of up to 8°C in the air cavity after vegetation and a reduction of an air temperature of up to 4°C. Perez et al. [28] analyzed the effect of green walls in a Mediterranean climate. Results confirm the ability of green walls to generate shade on the walls

Fig. 1. Modular vegetal façade system before and after the insertion of plants.

Fig. 2. Headquarter of innovation and technology for development centre (itdUPM) — madrid, Spain.

of buildings, and the relevance of the microclimate created in the cavity between the façade and the wall as well as within the building. It is important to emphasize that to study the behavior of green walls, variables, with the capacity of reducing temperature, must be considered. Different studies have shown the influence of the climate [35,36], system design and components [37], the irrigation and fertilization system [11], and the type of plants and substrate [17,38,39], both in terms of performance and environmental sustainability [40].

The majority of the studies carried out compare conventional façade solutions with vegetable façade systems, being analyzed in the same geographical context and under the same orientation. Tendentially, they are the most beneficial in terms of solar exposure according to the latitude in which the research is carried out. Therefore, the objective of the present study is to analyze the effect of vegetation on the reduction of surface temperatures under different orientations (south and west) in a Mediterranean climate, from the study of environmental variables such as irradiation and air temperature. Since the objective is to measure the influence of the irradiation on the thermal behaviour of vegetation and the possible reduction of temperatures in different layers of the façade, the following questions have been asked: Is the temperature reduction effect of a green wall affected by its orientation? Is there an important difference between the surface temperatures of a green wall and a metal envelope exposed to the south and west? Is irradiation a determining value in the effects associated with green walls?

The rest of the paper is as follows. Section 2 focuses on the Innovation and Technology for Development Centre building, where the vegetal façade under study has been installed. In Section 3, an exhaustive data analysis of the behavior of the vegetal façade is performed. Finally, Section 4 concludes the paper.

2. ITD building

The ItdUPM building at Universidad Politécnica de Madrid (UPM) was developed with the aim of creating the first building of almost zero energy consumption inside the campus. To comply with the thermal requirements of the new proposal, a retrofitting was made by adding materials such as glass wool to the existing walls for improving thermal transmittance. The building includes a drilled metal plate skin covering all the façades, leaving an air gap between the concrete wall and the mentioned skin of 20 cm. Additionally, some parts of the skin are covered by a green wall.

The ItdUPM makes use of passive strategies to reduce the energy consumption as well as the indoor thermal comfort. The integration of a green wall in the south (11.25m2), east (6.25m2), and west (10m2) façade was part of these strategies (see Fig. 2). The green wall installed is a modular system called BIOFIVER[1]. It is formed by two three-dimensional structures of polypropylene cells, separated by hydrophilic polyester fabric (see Table 1 for a detailed list of the components).[2] Specifically, the dimensions of each module is 50 cm × 50 cm x 10 cm. Additionally, the front structure is filled with organic substrate enriched for the cultivation of plants, that are selected based on their adaptation to the climate in which they are located. The plants selected for the ITD building are shown in Table 1. They are pre-cultivated and inserted in gaps. The rear structure remains empty, generating a hollow space for air circulation (see Fig. 3).

Moreover, the green wall has an exudation irrigation system that allows the entire surface to have the same amount of water at any point. This favors that the necessary irrigation for the green wall can be easy calculated. The number of plants installed per module is 16, i.e. 64 plants per m2.

A real-time distributed monitoring system has been installed to analyze the behavior of the south and west façades. The monitoring system is based on an ad-hoc designed embedded system connected through an RS-485 serial bus to several distributed nodes. These nodes are directly connected to eight type-T thermocouples (0.1 °C resolution), two pyranometers[3] (0.1 W/m^2 resolution) and one meteorological station.[4] The nodes are running a real-time operating system which takes care of acquiring all measurements at specific time frames. Every 10 ms. each node obtains information from all the sensors at which it is connected. Every second the monitoring node performs the mean of the last 100 measurements and stores it internally to be acquired by the main controller through an RS-485 RTU-Modbus protocol. The main controller is based on an embedded Linux operating system. It is made of

Table 1
Components of BIOFIVER system.

BIOFIVER system	
External finishing layer	Polyester
Bearing structure	Polypropylene boxes
Hidrophilic layer	Polyester
Growing medium	Coconut fibre, turf and hummus
Closing layer	Polyester
Hooking system	Aluminium
Vegetation layer	Hedera h., Carex, Flagellifera, Carex Testacea, Carex Oshimensis, Crassula radicans “Small Red”, Erigeron karvinskianus, Frankenia Iaevis, Helycrisum italicum, Heuchera americana, Lamium maculatum, Lampranthus aurantiacus, Lavandula dentata, Lavandula dentata, Lonicera nítida, Myrtus communis, Polygonum capitatum, Rosmarinus, Santolina chamaecyparissus, Sedeveria, Sedum álbum, Sedum palmeri, Sedum lineare, Thymus vulgaris

[1] https://igniagreen.com/sistema-vertical-para-paredes-vegetales/.

[2] http://vertiarte.com/sistemas-y-productos/modulos-biofiver/.

[3] LI-COR LI-200R

[4] David Vantage Pro2 Wireless.

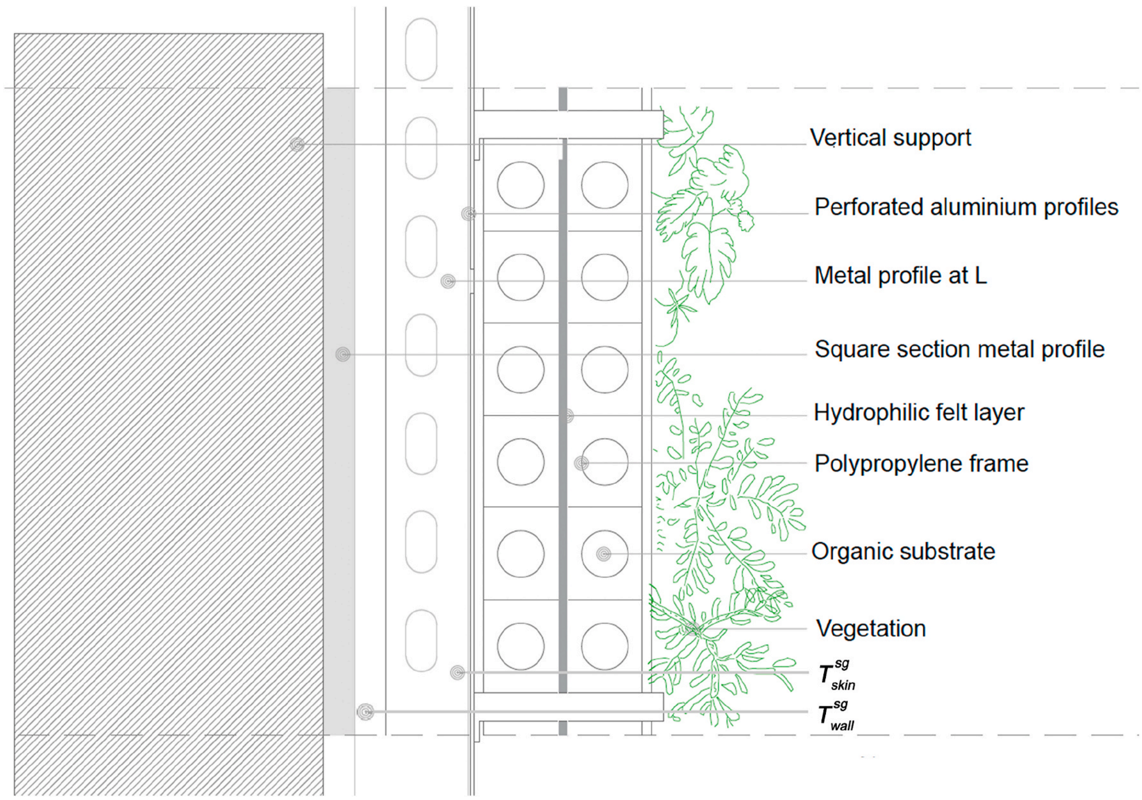

Fig. 3. itdUPM green wall section. (For interpretation of the references to color in this figure legend, the reader is referred to the Web version of this article.)

a microcontroller with a UPS system and an electronic carrier to connect to the nodes. Every minute, the main controller acquires all measurements stored on the nodes and accumulates them on an internal SD card. This information is stored together with the date and time. Moreover, every 5 min the main controller sends the data stored to the monitoring server. The monitoring server is in charge of synchronizing all data, performing all conversions from electrical to physical measurements and running periodic scripts which process the data and upload them to the monitoring database. A monitoring website has been created to allow researchers and the general public observe the behaviour of both façades in real time.[5] All the information presented in this manuscript is extracted from that website and is accessible to the general public. The data obtained to the analysis performed in Section 3 is gathered from June 2016 until September 2019, although monitoring is still ongoing. The time series data set is currently composed by more than 2 million of samples with 1 min sampling period.

Table 2
Table of absolute variables notation.

Absolute variables
T^{sc}_{skin} ≜ South façade skin temperature, control surface.
T^{sc}_{wall} ≜ South façade wall temperature, control surface.
T^{sg}_{skin} ≜ South façade skin temperature, green wall.
T^{sg}_{wall} ≜ South façade wall temperature, green wall.
T^{wc}_{skin} ≜ West façade skin temperature, control surface.
T^{wc}_{wall} ≜ West façade wall temperature, control surface.
T^{wg}_{skin} ≜ West façade skin temperature, green wall.
T^{wg}_{wall} ≜ West façade wall temperature, green wall.
T_{ext} ≜ Exterior temperature
I^{s} ≜ South façade irradiance on the vertical plane.
I^{w} ≜ West façade irradiance on the vertical plane.
H_{ext} ≜ Exterior humidity
UV ≜ UV index on the horizontal plane.
v_{wind} ≜ Wind speed

3. Exploratory data analysis

In this Section, a comparison between a control surface (the metal plate without the green wall) and the green wall is considered. Table 2 gathers the notation of the sensors under study (see Fig. 4).

Notice that subindex *skin* or *wall* represent that the sensor is located at the skin (metal plate with our without vegetation) or wall respectively. Superindex *s* and *w* denote south and west façades respectively. Moreover, superindex *c* denotes that the sensor is placed on the control surface, the metal plate without the green wall. On the contrary, superindex *g* indicates that the sensor is placed behind the green system.

Fig. 5 depicts a heatmap representing a simplified correlation matrix between temperatures and environment variables. UV and v_{wind} share a noticeably weak and almost negligible correlation with the temperature features, concluding that their impact on the green façade behavior is not significant. On the contrary, there is an outstandingly strong correlation in the case of T_{ext} and H_{ext}. While the former variable shows a similar correlation with all temperatures, in the case of the humidity, its impact is slightly less appreciable behind the green wall (temperatures with superindex *g*). Special attention is required in the first two columns of the matrix which collect the correlations with the irradiance in both façades. The first issue highlighted is the fact that, with exception of T^{sc}_{skin}, the south temperatures have a stronger correlation with the west façade irradiance compared to the south one. In the subsequent, some evidences supporting that the cause is a delay produced by the green wall in the temperature time series T^{sg}_{skin} with respect to T^{sc}_{skin} will be provided. Moreover, the mentioned delay causes a better curve fitting of

[5] http://monitoring.robolabo.etsit.upm.es/itd/.

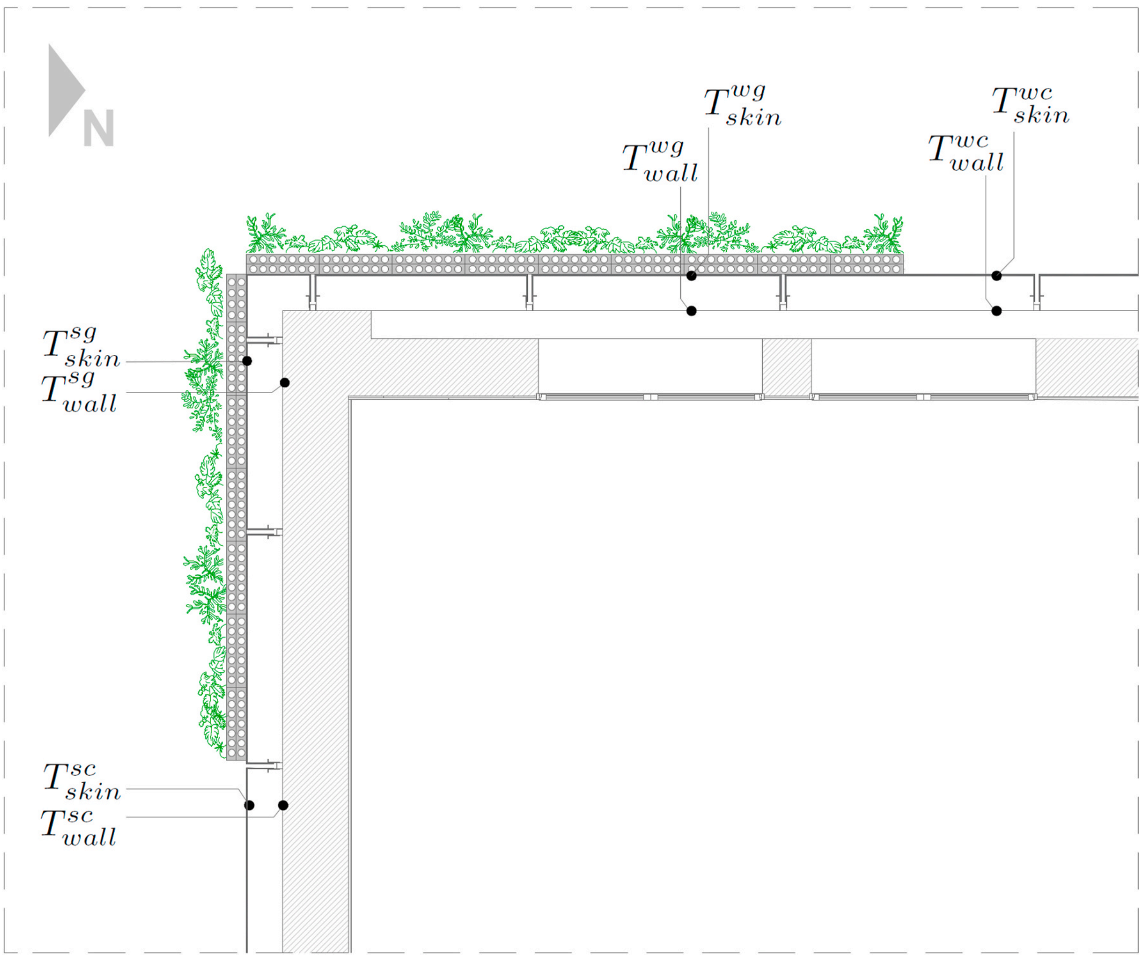

Fig. 4. South-west corner of the itdUPM bulding where all variables measured are displayed (see Table 2).

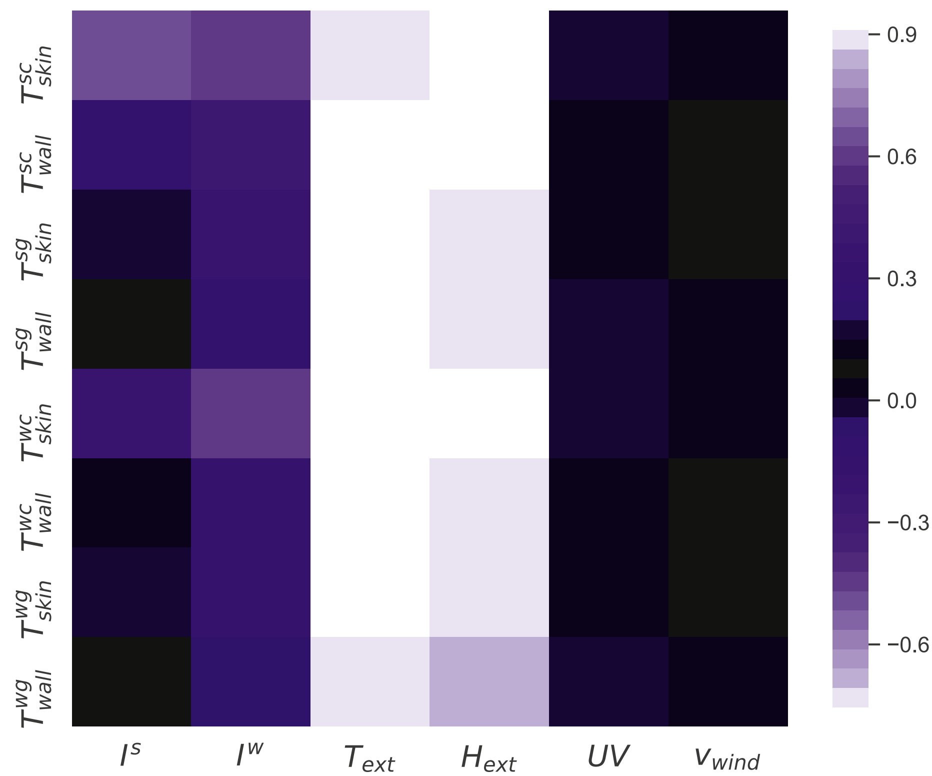

Fig. 5. Simplified correlation matrix between temperatures and the remaining potentially relevant features. Black denotes a weak linear correlation between the variables and white represents an outstanding strong correlation. In order to increase its interpretability, the same colors were used for strong correlation and strong anticorrelation. (For interpretation of the references to color in this figure legend, the reader is referred to the Web version of this article.)

T^{sg}_{skin} to I^w profile than to I^s (taking into consideration that the daily profile of I^w is also delayed with respect to I^s). This statement explains why the aforementioned correlations in the south areas with green wall are too weak when compared to I^s. Because of the strong dependence on temperature and irradiance, these two variables have been selected for the behavior data analysis.

Fig. 6 provides a better illustration of this phenomenon. The scatterplots relating control surface skin temperatures with irradiances in both south and west façades (Fig. 6a and c) denote an existing linear relationship between the targeted variables. On the contrary, a different situation can be observed in the scatterplots where green façade skin temperatures and irradiances (Fig. 6b and d) are compared. In this scenario, the scatterplots show a poor linear relationship between the variables in any of the studied façades. Although this observation could drive to the conclusion that the green wall is erasing the correlation between T^{sg}_{skin} versus I^s and T^{wg}_{skin} versus I^w, a deeper understanding of the wall behavior can be obtained by including the time factor in the analysis (see Fig. 7).

Fig. 7 plots the cross correlation between each temperature in south and west façades and their corresponding irradiance (I^s or I^w) using data samples of the summer. The correlation analyzed in Fig. 5 corresponds to the correlation for a zero lag or displacement ($\tau = 0$) in Fig. 7. The illustrated graphs have been obtained by means of the unbiased sample cross correlation estimator as follows: the time series is split into a set of non-overlapping segments of length 1440 (so that each segment is a different day with 1 min resolution of the time series). Subsequently, the unbiased sample cross correlation estimator between $Y(k)$ and $X(k)$, defined as in Equation (1), is applied to each segment. In this case, $X(k)$ is either I^s or I^w depending on the façade and $Y(k)$ is the temperature time series under assessment (see Fig. 7). It should be mentioned that, aiming to decrease the non-stationarity of the analyzed processes, all the segments have been subject to an standarization process. Furthermore, the partitioning procedure and the selection of data belonging to the same season and year have also been applied in order to deal with the non-stationarity issue.

$$\widehat{R}_{YX}(\tau) = \frac{1}{N-\tau}\sum_{k=0}^{N-\tau-1} Y[k+\tau]X[k], \quad \tau \in \{0, \dots, 1439\} \tag{1}$$

Fig. 7 depicts the sample mean and sample standard deviations of the cross correlation estimates of all segments. The most relevant part of Fig. 7 is the region of the function where the first cross correlation peaks are produced (τ values between 1 and 7 depending on the temperature sensor and the façade). This peak of correlation represents the delay between the temperatures and the irradiance. In the south area of the building, it can be highlighted that the peak of correlation between T^{sc}_{skin} and I^s is produced for a delay of 1 h, while T^{sg}_{skin} exposes a maximum for 3.5 h. Therefore, it is corroborated that a delay exists between the temperatures covered by the green wall and the irradiance at the corresponding orientation. Moreover, the black curve of Fig. 7a displays the direct cross correlation between T^{sc}_{skin} and T^{sg}_{skin}. In particular, the peak of cross correlation is approximately produced at a delay of 2.5 h. This observation leads to the conclusion that the green wall is generating a delay of about 2.5 h in the temperature of its skin surface. A similar scenario can be observed in the west façade, albeit the delays are less noticeable. This means that the green wall generates a positive effect on the outer layer of the building, providing a reduction in temperature and a delay in the maximum peak. Another remarkable observation is that the cross correlation curves of T^{sg}_{skin} and T^{sc}_{wall} with I^s in south (Fig. 7a) and T^{wg}_{skin} and T^{wc}_{wall} with I^w in west (Fig. 7b) are extremely similar. Therefore the delay produced by the green façade is comparable to the one caused by the air chamber between skin and wall surfaces.

Fig. 8 displays the daily profile of the temperature variables. In addition to the wall temperature measurements, the irradiance (black) and exterior temperature (green) are shown together. Focusing on the south façade, it can be observed that T^{sc}_{skin} is utterly high (for instance around 45°C in summer at 15:00). Furthermore, its thermal time

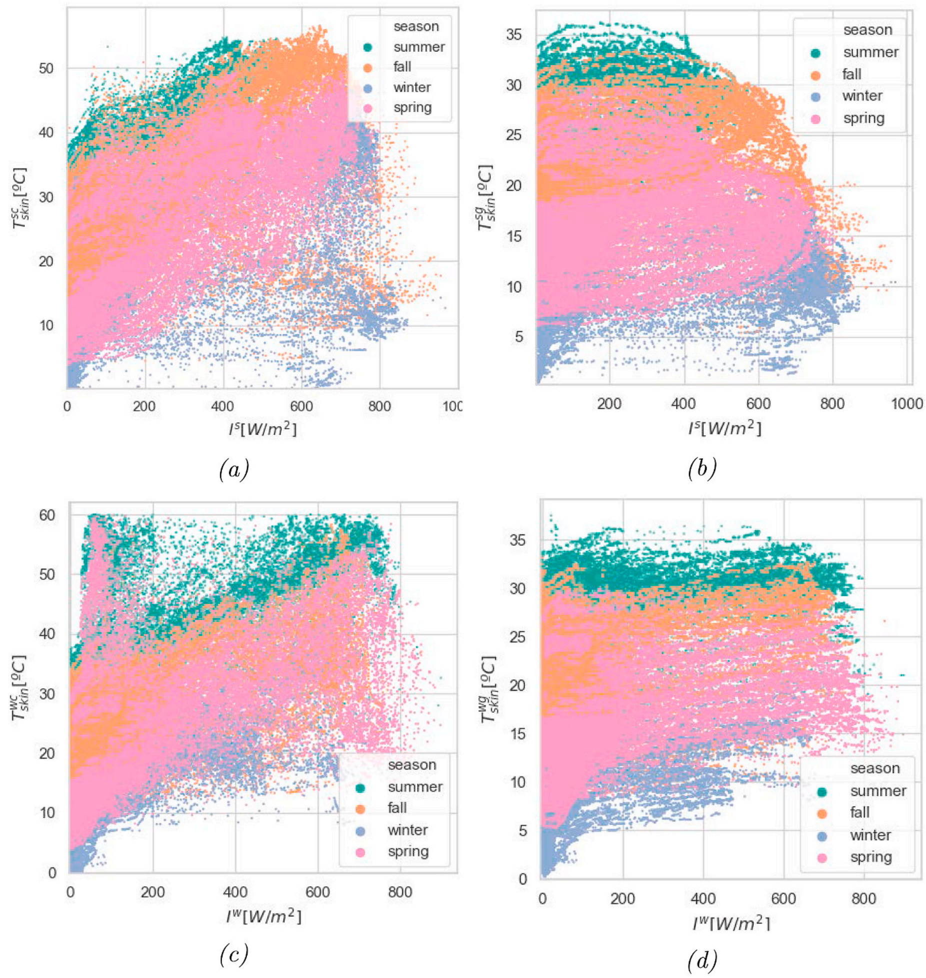

Fig. 6. Scatterplots of (a) south control skin temperature (T^{sc}_{skin}) and south irradiance (I^s), (b) south green skin temperature (T^{sg}_{skin}) and south irradiance (I^s), (c) west control skin temperature (T^{wc}_{skin}) and west irradiance (I^w) and (d) west green skin temperature (T^{wg}_{skin}) and west irradiance (I^w) for each season of the year. (For interpretation of the references to color in this figure legend, the reader is referred to the Web version of this article.)

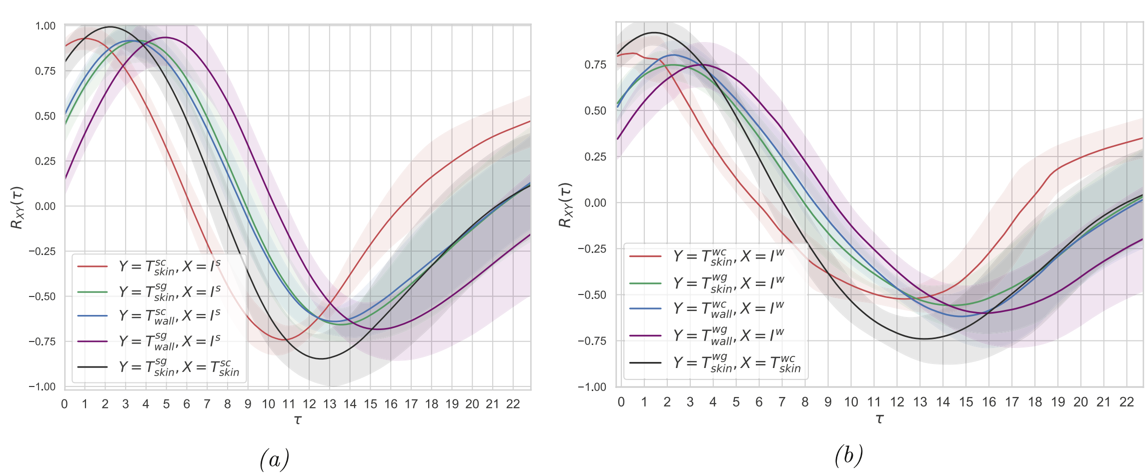

Fig. 7. Cross correlation functions of the temperatures and irradiance in (a) south façade and (b) west façade in summer 2018. Additionally, the black curves show the cross correlation function between control and green walls. The time series are partitioned into daily length segments. These segments are standarized and unbiased sample cross correlation is computed for each of them. In the curves, sample mean and sample standard deviation of each of the estimated cross correlations is depicted for each pair of variables. (For interpretation of the references to color in this figure legend, the reader is referred to the Web version of this article.)

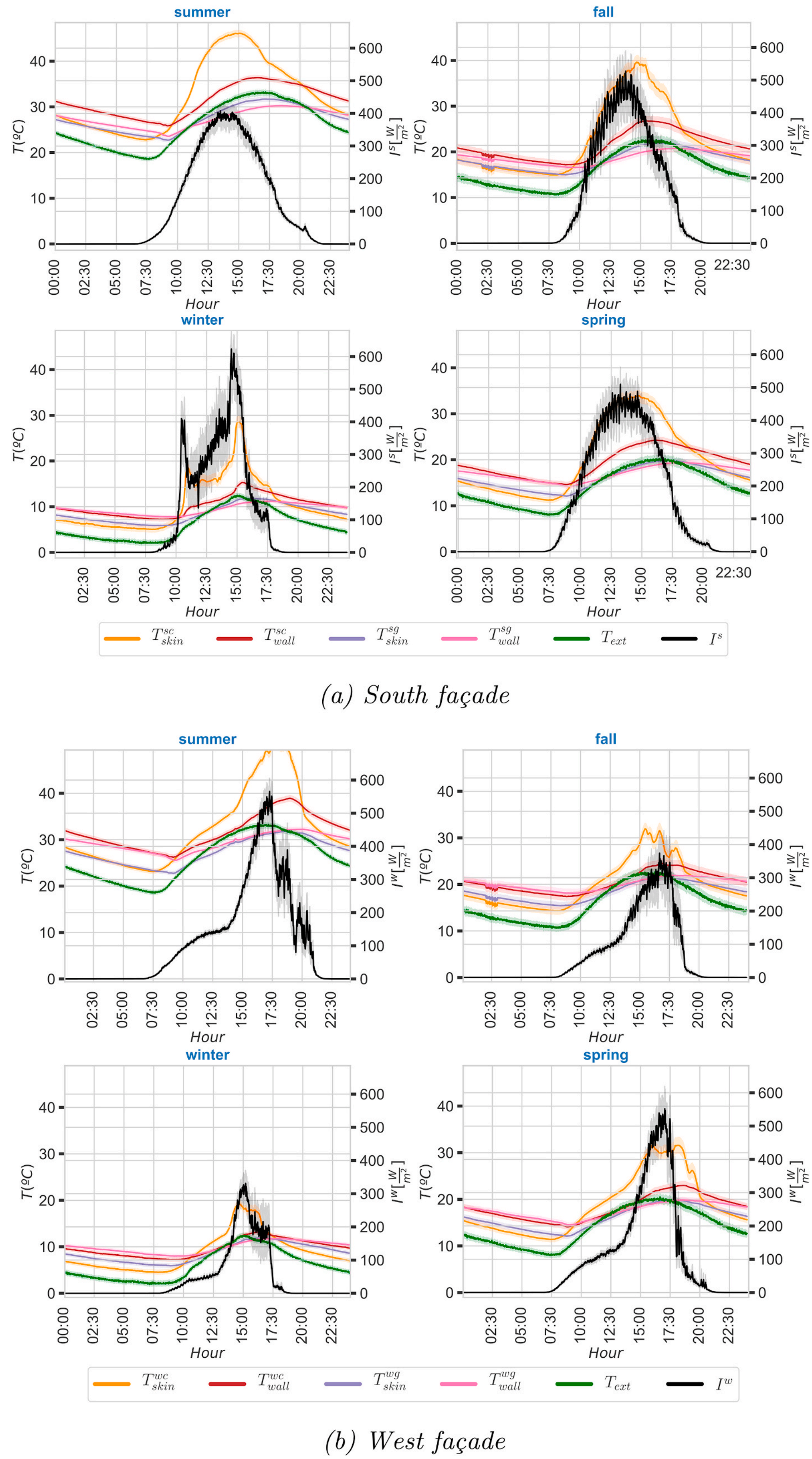

Fig. 8. Daily profile of temperatures in south (a) and west (b) façades of the building. The daily median of the temperature time series and its corresponding confidence interval with 95% of confidence level are represented for each minute of the day and for each season of the year.

constant is remarkably low [41], producing an almost simultaneous rise in temperature with the incident irradiance. Subsequently, the temperature T^{sc}_{wall} is substantially smoothed and suffers a delay of about 120 min (observing the time when the curves start to increase) and a decreased slope in the rising of the temperature in the morning, that can be interpreted as a low pass filter. Notice that the mentioned delay can be also observed in Fig. 7a) between between red and blue curves. Moreover, T^{sg}_{skin} (purple curve) is already smoothed with respect to T^{sc}_{skin} and its slope is even slower than T^{sc}_{wall}. Therefore, this fact suggests that the green wall is performing a similar low pass filtering as the air chamber between the control surface and the wall of the building in the control area. The final temperature measurable in the area of the façade with green wall is T^{sg}_{wall} (pink curve), that is comparable to T^{sg}_{skin} but with lower temperatures in midday and larger values during the night, being a desirable behavior. Thus, the green wall acts as a buffer of the external conditions, providing the building's skin with lower temperatures during the day when there is a greater need for cooling. At the same time, the green façade provides higher temperatures during the night, when the indoor temperatures tend to be lower due to the important thermal excursion that characterizes continental climates. As a consequence, the achieved daily profile of the Temperature T^{sg}_{wall} is noticeably flat, resulting in thermal stability in the outer skin of the building.

Looking at T^{sg}_{wall}, it can be observed that it has a similar daily profile to T^{sg}_{skin} but with lower temperatures during the day and barely larger values during the night. This behaviour can be explained considering that the wall is less exposed to the external conditions than the skin. Therefore, during the daytime, the effect of the irradiation produces a higher temperature on the skin area, whereas during the nighttime the exterior temperature affects the skin temperature more than the wall temperature. Thus, the use of an air chamber behind the vegetal cover seems to amplify the effect of the vegetation, resulting in greater thermal stability for the wall behind the green façade.

Furthermore, it is worth of highlighting the behaviour of the wall temperature behind the green façade (T^{sg}_{wall}, pink curve) in comparison with the wall temperature in the control surface wall (T^{sc}_{wall}, red curve). Fig. 8 shows that for all the seasons on both orientations, T^{sg}_{wall} is lower than T^{sc}_{wall}, being the differences highest in summer and fall (about 7 °C max.) and lower in winter (about 5 °C max.).

In addition to the absolute measurements, temperature differences (see Table 3) are calculated to compare how the green wall is working in comparison with the control surface at different orientations. Specifically, the difference between the skin and wall behaviors are compared both for the south (ΔT^{s}_{skin} and ΔT^{s}_{wall}) and west (ΔT^{w}_{skin} and ΔT^{w}_{wall}) orientations. These differences of temperature directly quantify how efficiently the green system is in terms of thermal protection compared to a control area in the same orientation. Fig. 9 depicts these variables for each season of the year. A remarkable fact is that during daytime there is a positive difference between south skin temperatures ΔT^{s}_{skin} (with maximum differences around 17°C depending on the season of the year), denoting that the sensor behind the green wall is measuring a lower temperature than the one on the control surface. Moreover, ΔT^{s}_{wall} maintains this positive difference but strongly attenuated. Even with this attenuation, the peak of ΔT^{s}_{wall} is between 5°C and 8°C depending on the season. This is an outstanding temperature reduction between the wall with and without green wall. On the contrary, results are less favorable during the night. During nighttime, wall sensors measure on average very poor temperature differences (ΔT^{s}_{wall}) that in most cases may not be noticeable. Winter, spring and fall seasons show values of $|\Delta T^{s}_{wall}|$ that are at most 1°C. In the case of summer season, the wall temperature differences are more important, measuring values between 2°C and 4°C. In regard to nighttime thermal performance of the green wall, west orientation shows even worse results because of the reduced values in summer (maximum of 2°C in midnight) with respect to south measurements.

Table 3
Table of temperature differences notation.

Temperature differences
$\Delta T^{s}_{skin} = T^{sc}_{skin} - T^{sg}_{skin}$, $\Delta T^{w}_{skin} = T^{wc}_{skin} - T^{wg}_{skin}$
$\Delta T^{s}_{wall} = T^{sc}_{wall} - T^{sg}_{wall}$, $\Delta T^{w}_{wall} = T^{wc}_{wall} - T^{wg}_{wall}$
Second order temperature differences
$\Delta^2 T^{sw}_{skin} = \Delta T^{s}_{skin} - \Delta T^{w}_{skin}$
$\Delta^2 T^{sw}_{wall} = \Delta T^{s}_{wall} - \Delta T^{w}_{wall}$

Therefore, the green wall allows reducing the incoming thermal loads during daytime in summer, fall and spring, performing as a very effective sun shading device. On the other hand, in winter and during nighttime its effects are greatly reduced. This is a positive conclusion as the reduced thermal loads in the warm periods do not correspond to an increase in thermal loads in the cold periods. Another issue to be remarked is the fact that the temperature differences are highly dependent on the irradiance profile, as shown in Fig. 9. This means that the green wall system reduces the wall temperature and thus the thermal load by conduction through the wall. In Fig. 9, it is also observable that, with the exception of the summer season, the differences of temperature are larger in the south orientation. Besides, it can be noted that during the summer the temperature reduction in the south façade occurs mainly in the central hours of the day, while in the west façade it occurs mainly in the afternoon, corresponding in both cases with the radiation profile in the two orientations. Being the summer the most relevant season for the use of green walls, this information allows the designers to predict at what time of day the façade provides a temperature reduction, depending on the orientation. This is useful when selecting the façade where the green wall will be placed, and that will depend mainly on the hourly profile of the building.

Therefore, a direct comparison in terms of temperature difference between south and west façades is carried out. The objective is to deepen into the dependency of the green wall placement with the temperature. Fig. 10 shows the daily profile of the variables $\Delta^2 T^{sw}_{skin}$ and $\Delta^2 T^{sw}_{wall}$, representing the comparison between temperature differences in south and west façades (see Table 3). More precisely, a positive value indicates that the south green wall is performing more suitably due to a lower temperature in its green wall area. It is shown that the green wall located in the south surface is more efficient than the one facing to the west between 10:00 and 15:00. On the other hand, the green wall performs better in the west façade between 15:00 and 20:00. This difference is mainly caused by the irradiance profile, whose peak is firstly produced in south and subsequently in west. This issue is also observable in Fig. 9, noticing that the peak of difference in each wall is produced at different instants of the day. One interesting issue to be pointed out is that, in winter and fall, $\Delta^2 T^{sw}_{skin}$ is always positive. Being the autumn and winter seasons of the year in which in the city of Madrid normally do not have refrigeration charges, it seems logical to conclude that during the cold seasons the south façade has better behavior than the west. Moreover, if the profile of $\Delta^2 T^{sw}_{wall}$ is observed, the west wall only behaves better in summer during the period of time between 17:00 and 20:30. This means that buildings that are mainly used in the afternoon or that have cooling loads that originate primarily in the west orientation, will be more

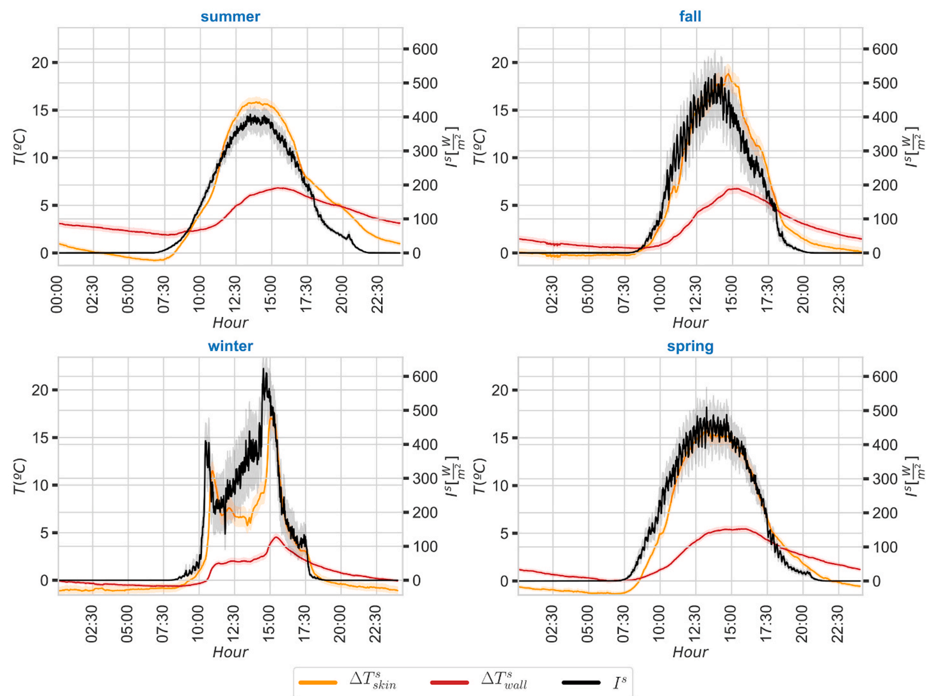

(a) South façade

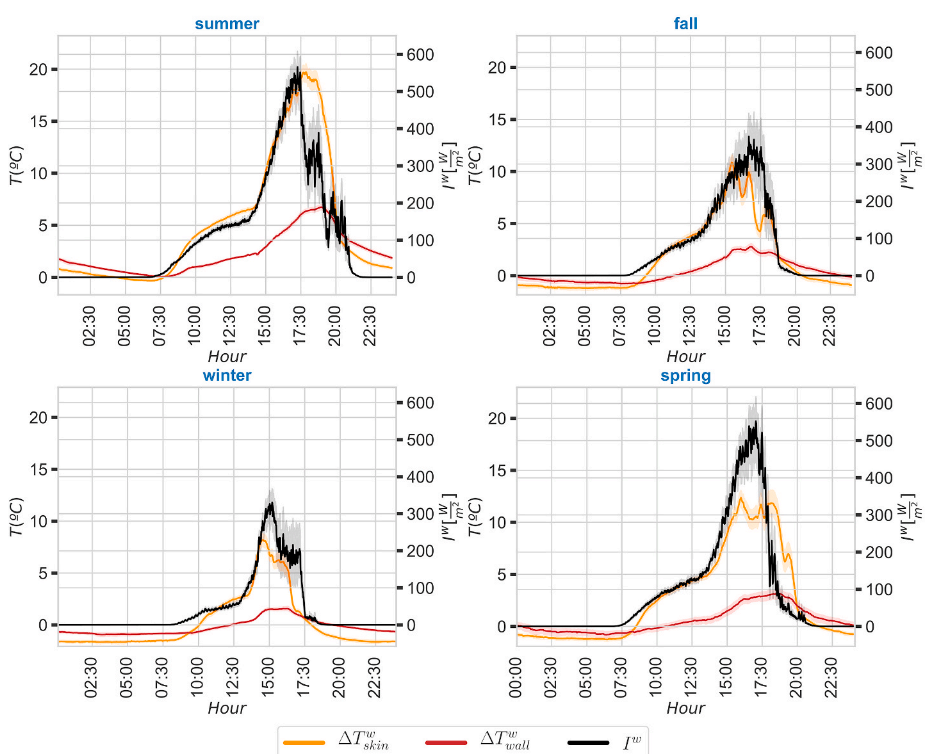

(b) West façade

Fig. 9. Daily profile of temperature differences in south and west façades of the building. The daily median of the ΔT time series and its corresponding confidence interval with 95% of confidence level are represented.

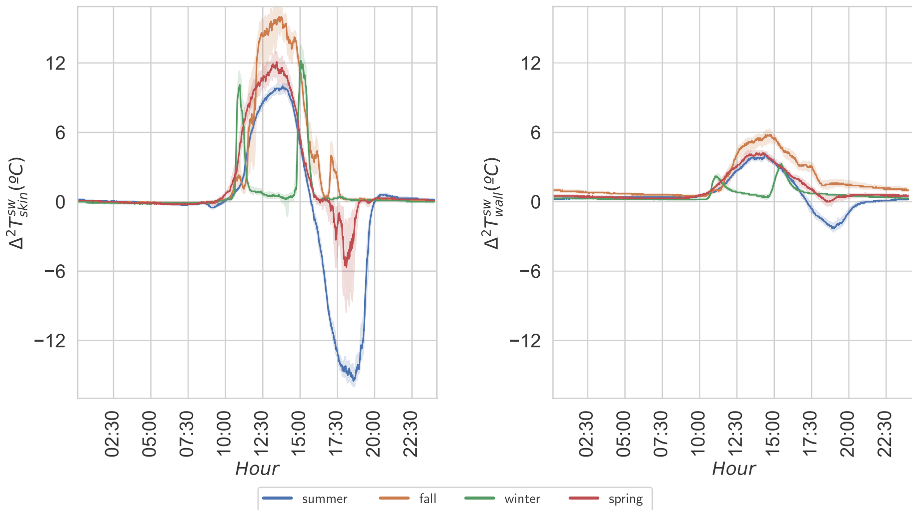

Fig. 10. Comparison of south and west façades by means of second order temperature differences (see Table 3) in skin (left) and wall (right). It depicts the median estimation during the day for each season with its corresponding confidence interval with 95% of confidence level.

favored by the installation of a green wall on the west façade. For the rest of the buildings, it seems logical to conclude that a green wall in the south façades behaves better than a green system in the west ones, at least during the hot seasons.

Finally, the previous observations and conclusions taken from Figs. 8 and 9 are formalized by means of hypothesis testing. In order to define the tests, let $T^{sc,i}_{wall}(k)$, $T^{sg,i}_{wall}(k)$, $T^{wc,i}_{wall}(k)$ and $T^{wg,i}_{wall}(k)$ be the south control, south green, west control and west green wall temperature random variables for season of the year i and minute of the day $k \in \{1,\dots,1440\}$. For instance, all the measurements of T^{sg}_{wall} performed in summer at 14:00 form a sample of the random variable $T^{sg,i}_{wall}(840)$. With this notation, Hypotheses 2 and 3 are proposed as the null hypothesis to be assessed for season i and minute k of the day in south and west façades respectively. μ_X is the population mean of the distribution X.

$$H_0^{i,k,south} : \mu_{T^{sc,i}_{wall}(k)} - \mu_{T^{sg,i}_{wall}(k)} = 0 \tag{2}$$

$$H_0^{i,k,west} : \mu_{T^{wc,i}_{wall}(k)} - \mu_{T^{wg,i}_{wall}(k)} = 0 \tag{3}$$

The starting point to validate or refuse the mentioned null hypotheses is to verify if the normality assumption was fulfilled for each sample. Therefore, Shapiro-Wilk test [42], which null hypothesis states that the underlying distribution of the sample is a normal random variable, is used. Owing to the fact that all the samples led to an extremely low p-value, the normality assumption of the data sample is rejected. Thus, a non-parametric hypothesis test is selected to decide on the validity of Equations 2 and 3. More precisely, Wilcoxon signed-rank test [43] is applied. With the aim of visualizing the results of all the tests in a compact way, a graph depicting the resulting $\log(p-\text{value}(k))$ for $k \in \{1,\dots,1440\}$ is presented in Fig. 11a for the south façade and in Fig. 11b for the west orientation. The black horizontal line shows the natural logarithm of the selected significance level of the tests. Thereby, the null hypothesis is accepted for those instants of the day when $\log(p-\text{value}(k))$ surpasses the horizontal line and rejected otherwise. Fig. 11a, shows that there is strong evidence to state that T^{sg}_{wall} is larger (see Fig. 9) than T^{sg}_{wall} during all the day in summer. The remaining seasons have just some periods of the day when $H_0^{i,k,south}$ is rejected (mainly between 11:00 and 21:00, corresponding to sun activity peak), highlighting the fact that fall is the season when the inequality of temperature means is less evident. On the contrary, the west façade tests results are less favorable. Even though summer tests are still rejected in almost all the instants of the day, the other seasons show a contrary scenario of p-values that provide strong evidences to reject the null hypotheses in shorter periods of time than in the south orientation.

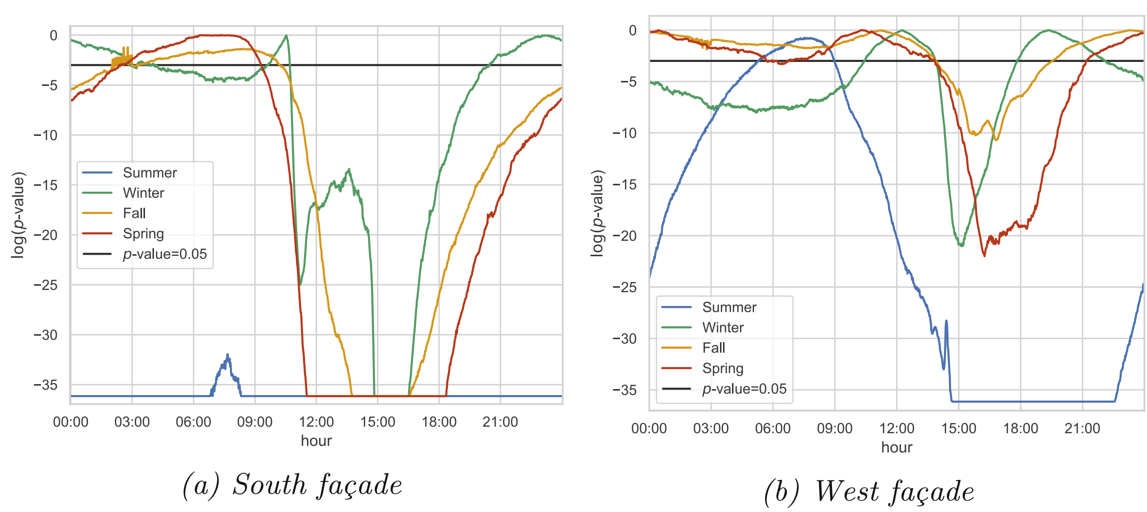

Fig. 11. Natural logarithm of the p-values obtained from the non-parametric hypothesis tests to verify hypotheses 2 and 3 on each minute of the day and each season of the year for south façade in (a) and west façade in (b). Null hypotheses are rejected if the corresponding p-value lies below the black line (corresponding to the logarithm of the significance level $\log(\alpha)$.).

4. Conclusion

A retrofitted building located in Madrid was used to assess the impact of green wall systems on the building temperature in different orientations. The building is equipped with a monitoring system that gathers the temperature measurements with 1 min time resolution in different points behind the green walls and control surfaces. Therefore, a total amount of 2 million samples was used to accomplish an exhaustive comparison between control and green wall in south and west orientations aiming to conclude if there is statistical difference on their measurements.

The statistical analysis led to the conclusion that, on average, the control temperature is greater than the green wall temperature with a maximum difference of around $20^{\circ}C$ in summer and $8^{\circ}C$ in winter in the south skin area and about $7^{\circ}C$ in summer and in $2^{\circ}C$ in winter in the south wall surface. Non parametric hypotheses tests on the equality of means supported this observations. Although the results are positive during the day, difference of temperature in wall surface during the night period is not significant in any season (with maximum absolute temperature differences of $1^{\circ}C$) except summer (wall temperature differences ranging between $2^{\circ}C$ and $4^{\circ}C$).

The statistical analysis also revealed that the impact of the green wall on temperature reduction is more significant in the south façade than in the west façade. In order to assess it, the differences of temperature between control and green façades in south and west orientations were analyzed. On average, south skin differences are noticeably higher during all the day in fall and winter seasons (with maximum differences between south and west of about $16^{\circ}C$ in fall and $12^{\circ}C$ in winter). Similarly, summer and spring skin measurements also show superior temperature differences (about $16^{\circ}C$ superior in summer and $6^{\circ}C$ in spring) between 10:00 and 17:00. However, in the period of time between 17:00 and 20:30, west orientation provides more favorable results of about $16^{\circ}C$ superior in summer and $6^{\circ}C$ in spring.

The results obtained indicate that the green wall acts as a buffer of the external conditions, providing the building's skin with lower temperatures during the day when there is a greater need for cooling. At the same time, the vegetation layer provides higher temperatures during the night, when the indoor temperatures tend to be lower due to the important thermal excursion that characterizes continental climates. As a consequence, the daily profile of the temperature in the external surface of the wall is almost flat, resulting in thermal stability in the outer skin of the building. Furthermore, the use of an air chamber behind the vegetal cover seems to amplify the effect of the vegetation, resulting in greater thermal stability for the wall. The study also shows that both for the south and the west façade, the reduced thermal loads in the warm periods do not correspond to an increase in thermal loads in the cold periods.

Focusing on the different behavior of the two façades, it can be noted that during the summer the temperature reduction in the south façade occurs mainly in the central hours of the day, while in the west façade it occurs mainly in the afternoon. Being the summer the most relevant season for the use of green walls, this information is very valuable as it allows the designers to know at what time of day the façade provides a temperature reduction, depending on the orientation. This is useful when selecting the façade where the green wall will be placed, and that will depend mainly on the hourly use profile of the building. The buildings that are mainly used in the afternoon or that have cooling loads that originate primarily in the west orientation, will be more favored by the installation of a green wall on the west façade. For the rest of the buildings, it seems logical to conclude that a green wall in the south façade behaves better than a green wall in the west one, at least during the hot seasons. The results obtained also demonstrate that in the cold periods the green west wall has a better behavior than the south one, as the shading power of the green wall does not affect the possible external thermal gains.

Acknowledgments

The authors are grateful to the Universidad Politécnica de Madrid and the Innovation and Technology for the Development Centre for providing the means and resources necessary for this research work. We also want to thank Vertiarte company for providing the technical information of the green wall system used in this research.

References

[1] United Nations, Cities and climate change: policy directions. https://unhabitat.org/sites/default/files/download-manager-files/Cities, 2011. (Accessed 20 December 2019). Online.
[2] D. Schröter, W. Cramer, R. Leemans, I.C. Prentice, M.B. Araújo, N.W. Arnell, A. Bondeau, H. Bugmann, T.R. Carter, C.A. Gracia, A.C. de la Vega-Leinert, M. Erhard, F. Ewert, M. Glendining, J.I. House, S. Kankaanpää, R.J.T. Klein, S. Lavorel, M. Lindner, M.J. Metzger, J. Meyer, T.D. Mitchell, I. Reginster, M. Rounsevell, S. Sabaté, S. Sitch, B. Smith, J. Smith, P. Smith, M.T. Sykes, K. Thonicke, W. Thuiller, G. Tuck, S. Zaehle, B. Zierl, Ecosystem service supply and vulnerability to global change in europe, Science 310 (5752) (2005) 1333–1337.
[3] I. Andrić, M. Koç, S. Al-Ghamdi, A review of climate change implications for built environment: impacts, mitigation measures and associated challenges in developed and developing countries, J. Clean. Prod. 211 (2019) 83–102.
[4] N.J. Paull, P.J. Irga, F.R. Torpy, Active green wall plant health tolerance to diesel smoke exposure, Environ. Pollut. 240 (2018) 448–456.
[5] United Nations, Sustainable development goals [Online; accessed 10 December 2019], https://www.un.org/sustainabledevelopment/sustainable-development-goals/, 2015.
[6] European Commission, Nature-based solutions & re-naturing cities [Online; accessed 5 October 2019], https://ec.europa.eu/newsroom/horizon2020/document.cfm?doc_id=10195, 2015.
[7] J. Klingberg, M. Broberg, B. Strandberg, P. Thorsson, H. Pleijel, Influence of urban vegetation on air pollution and noise exposure - a case study in gothenburg, Sweden, Sci. Total Environ. 599–600 (1) (2017) 1728–1739.
[8] K. Perini, M. Ottelé, S. Giulini, A. Magliocco, E. Roccotiello, Quantification of fine dust deposition on different plant species in a vertical greening system, Ecol. Eng. 100 (1) (2017) 268–276.
[9] F. Mayrand, P. Clergeau, Green roofs and green walls for biodiversity conservation: a contribution to urban connectivity? Sustainability 10 (1) (2018) 985.
[10] M. Solera-Jiménez, Green walls: a sustainable approach to climate change, a case study of london, Architect. Sci. Rev. 61 (1–2) (2018) 48–57.
[11] S. Charoenkit, S. Yiemwattana, Living walls and their contribution to improved thermal comfort and carbon emission reduction: a review, Build. Environ. 105 (2016) 82–94.
[12] K. Perini, M. Ottelé, E. Haas, R. Raiteri, Greening the building envelope, façade greening and living wall systems, Open J. Ecol. 1 (1) (2011) 1–8.
[13] M. Köhler, Green facades—a view back and some visions, Urban Ecosyst. 11 (4) (2008) 423–436.
[14] G. Pérez, J. Coma, I. Martorell, L.F. Cabeza, Vertical greenery systems (vgs) for energy saving in buildings: a review, Renew. Sustain. Energy Rev. 39 (2014) 139–165.
[15] M. Manso, J. Castro-Gomes, Green wall systems: a review of their characteristics, Renew. Sustain. Energy Rev. 41 (2015) 863–871.
[16] T. Safikhani, A.M. Abdullah, D.R. Ossen, M. Baharvand, A review of energy characteristic of vertical greenery systems, Renew. Sustain. Energy Rev. 40 (2014) 450–462.
[17] V. Serra, L. Bianco, E. Candelari, R. Giordano, E. Montacchini, S. Tedesco, F. Larcher, A. Schiavi, A novel vertical greenery module system for building envelopes: the results and outcomes of a multidisciplinary research project, Energy Build. 146 (2017) 333–352.
[18] F. Victorero, S. Vera, W. Bustamante, F. Tori, C. Bonilla, J. Gironás, V. Rojas, Experimental study of the thermal performance of living walls under semiarid climatic conditions, Energy Procedia 78 (2015) 3416–3421.
[19] B. Chun, J.M. Guldmann, Impact of greening on the urban heat island: seasonal variations and mitigation strategies, Impact Green. Urban Heat Island: Season. Var. Mitigation strategies 71 (2018) 165–176.
[20] L. Kleerekoper, T.B.S.M. Van Esch, How to make a city climate-proof, addressing the urban heat island effect, Resour. Conserv. Recycl. 64 (2012) 30–38.
[21] Y. Xing, P. Jones, I. Donnison, Characterisation of nature-based solutions for the built environment, Sustainability 9 (1) (2017) 1–20.
[22] N. Fernández-Bregón, M. Urrestarazu, D.L. Valera, Effects of a vertical greenery system on selected thermal and sound mitigation parameters for indoor building walls, J. Food Agric. Environ. 10 (3) (2012) 1025–1027.
[23] M. Taleghani, Outdoor thermal comfort by different heat mitigatio n strategies- a review, Renew. Sustain. Energy Rev. 81 (2) (2018) 2011–2018.
[24] J. Kim, D. Gu, H.Y. Kim, Effects of urban heat island mitigation in various climate zones in the United States, Sustain. Cities Soc. 41 (2018) 841–852.
[25] F. Olivieri, C. Di Perna, M. D'Orazio, L. Olivieri, J. Neila, Experimental measurements and numerical model for the summer performance assessment of extensive green roofs in a mediterranean coastal climate, Energy Build. 63 (2013) 1–14.

[26] C. Bartesaghi Koc, P. Osmond, A. Peters, Evaluating the cooling effects of green infrastructure: a systematic review of methods, indicators and data sources, Sol. Energy 166 (2018) 486–508.
[27] D.H.S. Duarte, P. Shinzato, C. dos Santos-Gusson, C.A. Alves, The impact of vegetation on urban microclimate to counterbalance built density in a subtropical changing climate, Urban Clim. 14 (2015) 224–239.
[28] G. Pérez, L. Rincón, A. Vila, J.M. González, L.F. Cabeza, Behaviour of green facades in mediterranean continental climate, Energy Convers. Manag. 52 (4) (2011) 1861–1867.
[29] P.M.F. van de Wouw, E.J.M. Ros, H.J.H. Brouwers, Precipitation collection and evapo(transpi)ration of living wall systems: a comparative study between a panel system and a planter box system, Build. Environ. 126 (2017) 221–237.
[30] M.I. Touceda, F. Olivieri, J. Neila, Energy efficiency of a pre-vegetated modular facade prototype, in: 27th International Conference on Passive and Low Energy Architecture, Librairie Wallonie-Bruxelles, Paris, France, 2011, pp. 733–738.
[31] C.Y. Jim, H. He, Estimating heat flux transmission of vertical greenery ecosystem, Ecol. Eng. 37 (8) (2011) 1112–1122.
[32] N.H. Wong, A.Y.K. Tan, Y. Chen, K. Sekar, P.Y. Tan, D. Chan, K. Chiang, N. C. Wong, Thermal evaluation of vertical greenery systems for building walls, Build. Environ. 45 (3) (2010) 663–672.
[33] M. Ottelé, K. Perini, Comparative experimental approach to investigate the thermal behaviour of vertical greened façades of buildings, Ecol. Eng. 108 (A) (2017) 152–161.
[34] T. Safikhani, A.M. Abdullah, D.R. Ossen, M. Baharvand, Thermal impacts of vertical greenery systems, Environ. Clim. Technol. 14 (1) (2014) 5–11.
[35] F. Olivieri, D. Redondas, L. Olivieri, J. Neila, Experimental characterization and implementation of an integrated autoregressive model to predict the thermal performance of vegetal façades, Energy Build. 72 (2014) 309–321.
[36] F. Olivieri, L. Olivieri, J. Neila, Experimental study of the thermal-energy performance of an insulated vegetal façade under summer conditions in a continental mediterranean climate, Build. Environ. 77 (2014) 61–76.
[37] C. Jim, Greenwall classification and critical design-management assessments, Ecol. Eng. 77 (2015) 348–362.
[38] A.M. Hunter, N.S. Williams, J.P. Rayner, L. Aye, D. Hes, S.J. Livesley, Quantifying the thermal performance of green façades: a critical review, Ecol. Eng. 63 (2014) 102–113.
[39] H. Yin, F. Kong, A. Middel, I. Dronova, H. Xu, P. James, Cooling effect of direct green façades during hot summer days: an observational study in nanjing, China using tir and 3dpc data, Build. Environ. 116 (2017) 195–206.
[40] V. Oquendo-Di Cosola, F. Olivieri, L. Ruiz-García, J. Bacenetti, An environmental life cycle assessment of living wall systems, J. Environ. Manag. 254 (2020) 109743.
[41] P. Tsilingiris, On the thermal time constant of structural walls, Appl. Therm. Eng. 24 (5) (2004) 743–757.
[42] S.S. Shapiro, M.B. Wilk, An analysis of variance test for normality (complete samples), Biometrika 52 (3/4) (1965) 591–611.
[43] F. Wilcoxon, Individual comparisons by ranking methods, Biometrics Bull. 1 (6) (1945) 80–83.